RESEARCH ARTICLE

Hybrid Transformer Network for Soil Moisture Estimation in Precision Irrigation

NEETHU MADHUKUMAR[1,4], **(Member, IEEE), ERIC WANG**[1,3], **(Member, IEEE),**
YVETTE EVERINGHAM[1,3], **AND WEI XIANG**[2,1], **(Senior Member, IEEE)**

[1]College of Science and Engineering, James Cook University, Cairns, QLD 4870, Australia
[2]School of Computing, Engineering and Mathematical Sciences, La Trobe University, Melbourne, VIC 3086, Australia
[3]Agriculture Technology and Adoption Centre, James Cook University, Cairns, QLD 4814, Australia
[4]Department of Electrical and Computer Systems Engineering, Monash University, Melbourne, VIC 3800, Australia

Corresponding author: Neethu Madhukumar (neethu.madhukumar@my.jcu.edu.au)

ABSTRACT Accurate root zone soil moisture (RZSM) estimation is essential for precision irrigation (PI) systems that seek to optimize water use efficiency. Large-scale in-situ sensors for direct measurement are costly, while existing satellites lack depth resolution for direct RZSM data. Hence, in-direct RZSM estimation methods are required. Literature illustrates that RZSM at a location is related to changing soil-water-plant characteristics. Therefore, these characteristics can provide auxiliary information on RZSM changes. By leveraging auxiliary information derived from changing soil-water-plant characteristics, this paper enables indirect RZSM estimation at non-sensor locations, effectively addressing the limitations inherent in direct RZSM measurement techniques initially discussed. Compared to existing methods, deep learning (DL) is most suitable for such data associations as they are auto-tuned to extract relative relationships from diverse big data. Among DL models, sequential models are apt for finding these relationships as all these variables are time-series sequences. The transformer neural network (TNN) is the state-of-the-art DL model for analyzing sequences. However, for in-direct RZSM estimation, the data associations within a location and multiple sensor sites with the target need to be found. Conventional TNN cannot incorporate such simultaneous multi-associations, hence, we develop a new TNN model called the hybrid TNN model, which is able to facilitate the capturing of complicated dependencies through thoughtful feature selection and engineering. First, sensor locations exhibiting analogous downscaled 1-km satellite soil moisture (SM) are identified. Next, a dynamic multilayer perceptron (D-MLP) network discerns highly correlated auxiliary-RZSM data, utilizing both ground-based and downscaled satellite data. Following this, the dual attention module identifies essential multi-associations, leveraging selected sensor and target region information. Finally, the Bayesian layer averages multi-location RZSM using the conditional probability generated based on relative relationships to yield the target location RZSM estimate. Our proposed model shows 13.066% better RZSM estimation compared to popular sequential models. The hybrid TNN RZSM estimates are used to monitor root water depletion tolerance levels for optimal PI schedules, which shows 10.846% water and 10.339% cost-saving on our selected sites. Overall the proposed model effectively demonstrates that a more accurate PI predictive algorithm saves water, improves resource conservation, and reduces irrigation costs.

INDEX TERMS Agriculture, deep learning, hybrid transformer neural network, precision irrigation, root zone soil moisture.

I. INTRODUCTION

The root zone soil moisture (RZSM) is an indicator of the vegetation drought stress and the crop water demand, which

The associate editor coordinating the review of this manuscript and approving it for publication was Frederico Guimarães.

are valuable information for precision irrigation (PI) [1], [2]. In-situ sensors installed at root zone-specific depths can provide direct field RZSM measurements [3]. However, the vast installation of sensors across the field at the subsurface for RZSM measurements is not economically viable. Current satellite missions can provide kilometers of

distributed horizontal spatial details, but only centimeters of vertical (depth) SM information [4], [5], [6]. This vertical resolution can only provide knowledge of the surface soil moisture (SSM) layer, not the RZSM layer.

The limitations in direct RZSM measurements from in-situ sensors and satellite missions are predominantly addressed by indirect estimation through analytical methods using theoretical or empirical models to obtain fine-scale RZSM [7], [8]. These analytical methods use the relationship between environmental variables, such as precipitation, temperature, soil, and plant characteristics (PTSPc) which determines the RZSM state for indirect estimations [9]. However, these in-direct methods require in-situ (e.g. sensor) and ex-situ data (e.g. satellite) to improve the model's location-specific RZSM simulation accuracy [10]. Adoption of data-based methods can help remove these location-based optimization constraints as they are adaptive to data [11], [12], [13]. Among data-based methods, deep learning (DL) is becoming increasingly popular due to its deep architectures, which can extract accurate information from big environmental data [14], [15].

The application of DL in the realm of RZSM is still in the nascent stages [16], [17], [18]. However, RZSM is SSM diffused to lower soil layers [1], [19]. Consequently, the more advanced DL-based techniques for detailed SSM information, such as perform downscaling (increasing spatial/temporal details) by correlating the SSM with auxiliary SSM information available at target location [20], [21], [22], [23], can be extended to RZSM. Stream flow, another significant environmental parameter, exhibits remarkable similarities with moisture distribution within the root zone [24], [25]. Both parameters offer insights into the time-series movement of water, albeit within different mediums. Just as auxiliary information-based DL models have proven effective in the SSM domain, we can apply similar knowledge and methodologies from existing DL research in stream flow to enhance our comprehension of RZSM [25]. In instances where RZSM source information (whether in-situ or ex-situ) is scarce or unavailable, the environmental variables governing RZSM state can serve as valuable auxiliary information for these DL models. The literature suggests that employing a sequential DL model would be well-suited for conducting such correlation analyses [26], [27].

The transformer neural network (TNN) is the state-of-the-art DL model to process sequential data [25], [28]. It is a new cognitive model eschewing recurrence implementations in the previous benchmark sequential DL models, such as Long short-term memory (LSTM) [29] and Gated recurrent unit (GRU) [30]. LSTM and GRU receive the input information indirectly as a set of hidden states passed on through multiple cells via series processing. While, TNN can pay attention to every single input directly through parallel processing and attention mechanism to draw global dependencies between input and output. The attention mechanism enhances critical parts of the input while diminishing others so that the network

can devote more focus to the essential information [31]. The indirect RZSM estimation requires data from multiple sensor locations to be perceived simultaneously to draw critical information from target prediction. Hence we find TNN more suitable for RZSM estimation.

Furthermore, the LSTM and GRU-based RZSM works mainly focus on estimating RZSM using meteorological variables alone [27], [32]. However, other environmental variables also affect the RZSM state and should be considered for estimation. Unlike LSTM and GRU, more variables will enhance TNN learning due to parallel processing and attention mechanism [33]. Also, existing RZSM works aim at future predictions of a target location where ground truth is available [27], [32]. However, the main problem in the RZSM domain is the limited information on depth at locations without ground truth due to the shortcomings of direct measurement by in-situ and satellite devices. Such measurement constraints were addressed in the SSM domain using auxiliary variables correlations with the prediction target [20], [21], [22], [23]. This correlation approach is extrapolatable to the RZSM domain due to similarities with the SSM. In order to extrapolate the correlations from sensor location RZSM and auxiliary data for prediction at a site without direct measurement, we introduce a hybrid TNN model. We use auxiliary-RZSM variables identified in the literature for RZSM estimation: SSM, soil type, surrounding RZSM, target distance, plant type, RZSM depth, root type, plant daily water requirement, humidity, temperature, rainfall, soil salinity, and soil temperature [1], [9], [19], [27], [32].

In the proposed model first, as a high-level input abstraction, sensor locations with similar satellite SSM values as the target are selected for further analysis. To distinguish the SSM information from different test locations for similarity assessment, we use the downscaled 1 km SM from [34]. Next, a dynamic-MLP (D-MLP) finds the prominent PTSPc predictor variables from chosen sensor locations by determining the relative importance of these variables as a function of the neural network synaptic weights. The network assigns higher weights if the variables contribute more to the predictions. The selected sensor RZSM and auxiliary variables from the sensor and target locations are input to the attention layer of the proposed hybrid TNN model for further processing.

The attention block first analyses the relative relationship between the auxiliary variables at sensor and target locations. Next, the model performs a similar relationship analysis between sensor location auxiliary variables and RZSM. To achieve these proposed dual relative relationship analyses we concatenate an additional attention block to the basic TNN architecture. Inside the additional block, we implement a new multi-cross attention mechanism, which simultaneously analyses cross relative relationships between features from multiple sensor sites with the target. Unlike the conventional attention block, which transforms the output using its inputs, this block transforms the input using the inputs from the other concatenated block. Such an arrangement helps correlate the similarities of RZSM-related environmental changes
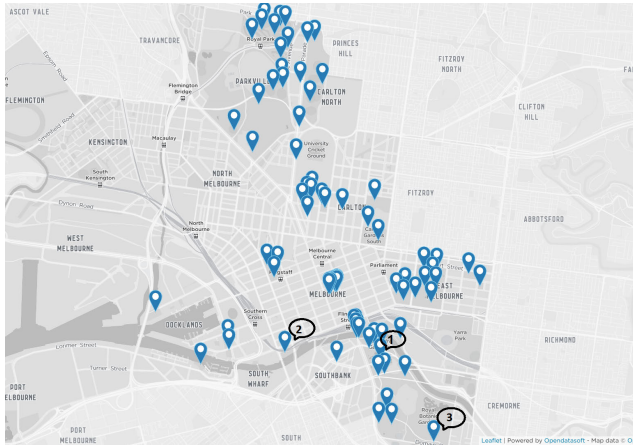
FIGURE 1. The study area map illustrates the distribution of 78 soil sensors across the city of Melbourne. The selected prediction sites are labeled as 1, 2, and 3: Alexandra Garden (1), Batman Park (2), and Fawkner Park (3). At these three locations, Root Zone Soil Moisture (RZSM) levels are predicted in-directly by inputting sensor data from all other locations on the map into the Hybrid Transformer Neural Network. The model's estimated RZSM values are then validated using RZSM data from the target prediction locations (labeled as 1, 2, and 3 on the map).

between target and selected sensor locations. Based on these relationships, probabilities were generated by the proposed hybrid TNN using the Bayes theorem in an additional layer implemented as a preceding layer to the traditional TNN output layer for each selected sensor RZSM. Finally, the probabilistic weighted sum of the selected RZSM sensors provides the required indirect estimates. A probabilistic weight assignment can reduce the uncertainties in multi-source ensembling [35] and can enhance the proposed model prediction accuracy as it combines multi-sensor data.

Based on the hybrid TNN RZSM estimates, we simulated PI schedules for the test locations for further evaluation. The proposed hybrid TNN model is compared with TNN [25], LSTM [27] and GRU [32] based related works for performance evaluation. A comparison of irrigation scheduling with these three models using quantitative measurements is conducted for the amount of water saved. These evaluations and comparisons will provide new insights for improvements in the RZSM estimation. The main contributions of this paper are summarized as follows:

1) A novel hybrid transformer neural network is designed to create a more discriminative extraction of auxiliary-RZSM variables for daily in-direct RZSM estimation.
2) A new deep learning-based method is proposed to fuse climate model outputs with satellite and ground-based data to aid in PI scheduling without requiring the large-scale installation of in-situ sensing stations.
3) A new deep learning-based decision support system for PI is developed to reduce irrigation water loss.
4) Proposed method produces highly accurate RZSM estimates across multiple root depths and when integrated as part of an intelligent PI automation system aids in water and cost-saving irrigation schedules compared to state-of-the-art neural network-based approaches.

The remaining paper is organized as follows: the study area and proposed model are elaborated in Section II. The simulation results are shown in Section III. Finally, a conclusion is drawn in Section IV.

II. MATERIALS AND METHODS

In this section, we introduce a novel hybrid TNN model for indirectly estimating RZSM, with the objective of enhancing PI decision-making. To evaluate the proposed model's performance, we will conduct a comparative analysis against hybrid-GRU [27], LSTM-Technique [32], and Multi-head TNN [25] within an irrigation framework. Both hybrid-GRU [27] and LSTM-Technique [32] predict RZSM using a sequential DL model, incorporating multiple auxiliary-RZSM variables as input to make informed irrigation decisions. Multi-head TNN [25] is a recent auxiliary variables-based prediction model. These comparisons will provide a benchmark for the proposed hybrid TNN-based RZSM estimation accuracy when compared to conventional TNN, LSTM, and GRU. Hence, we find these works highly valuable for comparison.

To facilitate a meaningful comparative analysis, the configuration of the comparison models, namely hybrid-GRU, LSTM-Technique, and Multi-head TNN, strictly follows the specifications outlined in the respective literature [25], [27], and [32]. Additionally, the configuration of our proposed model is detailed in Section II-B. To ensure a fair comparison, all competing models are provided with the same input variables (detailed in Section II-A) as those for the proposed model. However, since these input variables are measured in different units (for example: temperature in degrees Celsius, precipitation in mm/day, etc.), they are re-scaled into [0, 1] using Min-Max normalization as a pre-processing step. This ensures that all input features are treated equally in the learning process by all four models.

Finally, the Nash Sutcliffe coefficient of efficiency (NSE), determination coefficient (R2), and normalized mean bias error (NMBE) will be used to compare the performances of the four models. The subsequent section describes the study area, dataset, and input variables used in this study.

A. STUDY AREA AND DATASET

To test our proposed model we require a dataset having multiple RZSM sensing station readings installed over a vast spatially distributed area having similarities in the soil-plant-atmosphere domain. Hence we use the City of Melbourne (Australia) Soil Sensor Readings (CoMSSR [36]) dataset. The CoMSSR dataset contains historical readings for RZSM sensors and related auxiliary-RZSM variables within parks across the city of Melbourne. The units and readings at eight soil depths (0-80 cm) from 78 soil sensors installed locations are included within the CoMSSR dataset. The Soil Sensor Locations (SSL) dataset can be used to get the locations (latitude and longitude) where soil sensors have been deployed across the city. The CoMSSR dataset is joined to the SSL dataset [37] using the site-id column. The SSL

(a) Alexandra Garden, Melbourne　　　(b) Batman Park, Melbourne　　　(c) Fawkner Park, Melbourne

FIGURE 2. The layout of the three test sites: (a) Alexandra Garden (5.2 hectares) is located at 37.82037°S 144.971938°E with clay loam soil. It has an avenue of oak trees around the garden; (b) Batman Park (1.47 hectares) is located at 37.821766°S 144.956348°E with medium to heavily textured clay plus some sand. The park consists of sparse maturing eucalyptus trees with no understorey or saplings, and (c) Fawkner Park (41 hectares) is located at 37.838434°S 144.981016°E with sandy loam soil. The park has elm, oak, and fig trees.

dataset information can be further used to link with the soil type by area maps (STBAM) dataset to get the soil type information [38]. The CoMSSR, SSL, and STBAM datasets can be accessed for hourly values from the city of Melbourne-open data portal (https://data.melbourne.vic.gov.au/). The model is tested using data from June 2020 to February 2021, while the remaining 1 year and 2 months of data (preceding June 2020) from the CoMSSR, SSL, and STBAM datasets are used for training purposes.

The latitude and longitude information from the SSL dataset can be used to obtain the weather data from the nearest weather station accessible through the Bureau of Meteorology (BOM), Australia (http://www.bom. gov.au/). The weather station number from BOM can be used to join with the BOM forecast dataset [39]. The SSL dataset is further used to generate the fine resolution SSM for the 78 sensor locations. The fine resolution SSM is generated using the 9 km Soil Moisture Active Passive (SMAP) and 1 km Moderate Resolution Imaging Spectroradiometer (MODIS) satellite data, which can be accessed from NASA earthdata (https://search.earth data.nasa.gov/search). The sensor locations can be mainly classified as dry and wet regions. The Alexandra Gardens and Batman Park are wet regions as they are located near the Yarra River. Fawkner Park represents the case of a dry location far from any water bodies. Furthermore, these three test locations have the most widely available soil types in the world [40]. Hence our model is tested at these three locations illustrated in Fig. 2. The proposed model is elaborated further.

B. MODEL DESIGN

Fig. 3 illustrates the framework of the proposed decision support system for precision irrigation (DSS-PI). The proposed DSS-PI is made of three parts: 1) the SSM similarity assessment, 2) the RZSM estimation, and 3) the irrigation processor. Each part of the proposed DSS-PI is detailed below.

1) SSM SIMILARITY ASSESSMENT

Satellite imagery is made up of pixels and it represents the relative reflected light energy recorded for that part of the image. Each pixel represents a square area on an image and is a measure of the sensor's ability to resolve ground objects. The reflected energy from a light spectrum will be the same for objects that are similar in composition. Currently, satellites can only provide SSM information. Since SSM and RZSM are correlated, a similarity assessment of satellite pixels can help identify similar pixel-valued sensor sites with the target location without a sensor to further derive RZSM information.

A minimum of 1 km resolution is required to distinguish the SM pixels from the sensor sites in the CoMSSR dataset [36]. Currently, SMAP provides the highest resolution global daily SM of 9 km. Since this resolution is not sufficient for our application we downscale the 9 km SMAP SM to 1 km using the 3D-Bi-LSTM model [34] from our previous work. The target location 1 km downscaled SM is evaluated to check the overall similarity with all the sensor location's 1 km SM. Based on the SSM similarity sensor locations are selected. In order to identify the most important pixels that can contribute to the target prediction and reduce the complexity of analysis, we select pixels with at least fifty-percent similarity to the target. Next, the selected location features are passed on to hybrid TNN for further analysis.

2) RZSM ESTIMATION

Fig. 4 illustrates the proposed RZSM estimation using the hybrid TNN model. The D-MLP network forms the first processing layer of the proposed neural network. In the D-MLP the number of neurons is dynamically set at each cycle based on the similarity assessment in the current iteration. This design helps to analyze all locations with high similarity scores for any selected time rather than limiting the analysis to a fixed number of sites. Also, for locations with similar similarity scores, the closer in the range locations are given higher weights. This weight allocation is because closer regions to the target will have more similar environmental conditions. Hence the D-MLP hidden layer weights are further tuned based on the range value from the target location.

The calculation of whether a sensor is close or far in the distance (d) is performed using the longitude and latitude of the target point and $g \in \{1, 2, 3, \ldots, G\}$ selected sensor locations. The closest regions will have similar hydrological cycles compared to the farther located sensors. Hence the

Static Information

Dynamic Information

Output

DSS-PI Model
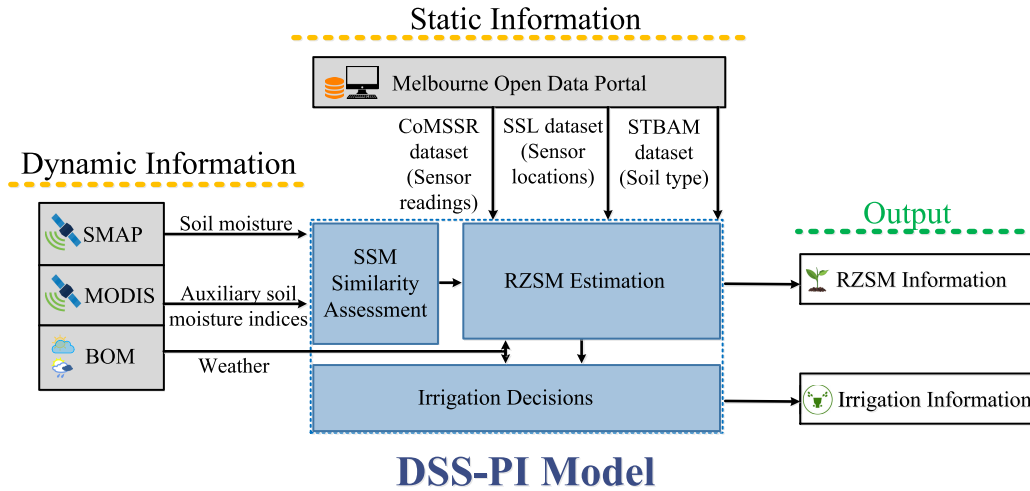
FIGURE 3. The framework of the decision support system for precision irrigation (DSS-PI). The dynamic information (SMAP, MODIS, and BOM) and static (CoMSSR, SSL, and STBAM) information are given as input to the proposed DSS-PI to get RZSM and irrigation information. First, the DSS-PI performs SSM similarity assessment using SMAP and MODIS data for selecting sensor locations for further analysis. Next, the RZSM estimation module outputs RZSM information using CoMSSR, SSL, STBAM, and BOM data. Finally, the irrigation processor provides the irrigation information using predicted RZSM and BOM rainfall data.

D-MLP assigns more weight to the decisions made from the information from closer sensor locations ($W_p > W_q \ \forall \ d_p < d_q$ if $p \neq q$).

Once the D-MLP weights are optimized, I auxiliary-RZSM information $f_g^i \in \{f_g^1, f_g^2, \ldots, f_g^I\}$ from the g selected similar locations are passed on to the D-MLP for finding the prominent auxiliary-RZSM information features. The D-MLP determines the relative prominence [41] of the predictor variables as,

$$V_{ij} = \sum_{k=1}^{K} W_{ik} \bullet W_{kj}, \quad (1)$$

where V_{ij} is the relative importance of any input variable f_g^i with respect to $j \in \{1, 2, \ldots, J\}$ output neuron (for J number of output neurons), K is the number of neurons in the hidden layer, W_{ik} is the synaptic connection weight between the input neuron i and the hidden neuron k, and W_{kj} is the synaptic weight between the hidden neuron k and the output neuron j. The D-MLP selects the top-ranked features, denoted as $I/2$, from the relevant list of I total predictor variables extracted from selected sensor locations, and forwards them to the attention module for root zone soil moisture (RZSM) prediction. Within the attention module, the multi-head attention component is dedicated to capturing dependencies within the input sequence, while the multi-head environmental inter-similarity attention component specifically focuses on identifying similarities and patterns across different sensor locations, thereby enhancing the model's environmental understanding.

The output of the multi-head attention module comprises attention weights assigned to each feature in the input sequence, facilitating the model's ability to concentrate on pertinent information while disregarding noise or irrelevant data. Similarly, the output of the multi-head environmental

inter-similarity attention module captures environmental similarities and patterns across various sensor locations, aiding the model in comprehending the broader environmental context.

By assimilating insights from the environmental inter-similarity, the model can generalize across diverse sensor locations and adjust its predictions based on the broader environmental context. Leveraging the outputs from the attention module, the proposed model executes a Bayesian averaging technique [35] on selected sensor location moisture data to predict the target RZSM accurately.

To calculate the probability values to perform the Bayesian average of the RZSM from selected sensors, first, the cross attention layer of the hybrid TNN evaluates the percentage similarity of features at the target location and selected sensor locations. Let $f_g^s \in \{f_g^1, f_g^2, \ldots, f_g^S\}$ be the D-MLP selected prominent features, where $S = I/2$ is the number of chosen features. The f_g^s is encoded as c_g^s through position encoding [42]. At a gth location, the SM can be expressed as a function of $s \in \{1, 2, \ldots, S\}$ prominent auxiliary-RZSM variables c_g^s,

$$y_g(t) = z_{P_g}\left(\sum_{s=1}^{S} c_g^s(t)\right) \forall t \in \{1, 2, 3, \ldots, T\}, \quad (2)$$

where z_{P_g} is the mapping function for the given hybrid TNN predictor neuron P_g. Eq. (2) gives the RZSM at a gth sensor location. However, we aim to find the RZSM at location $h \neq g$ without sensor. Hence we estimate $y_h(t)$ through Bayesian average of RZSM from g sensor locations. To estimate this, the relative relationship between the independent variable $c_g^s(t)$ at each gth location and $c_h^s(t)$ at target location 'h' needs to be derived. The proposed hybrid TNN's inter-similarity attention layer queries how related the encoded feature c_h^s at the target location is to the same
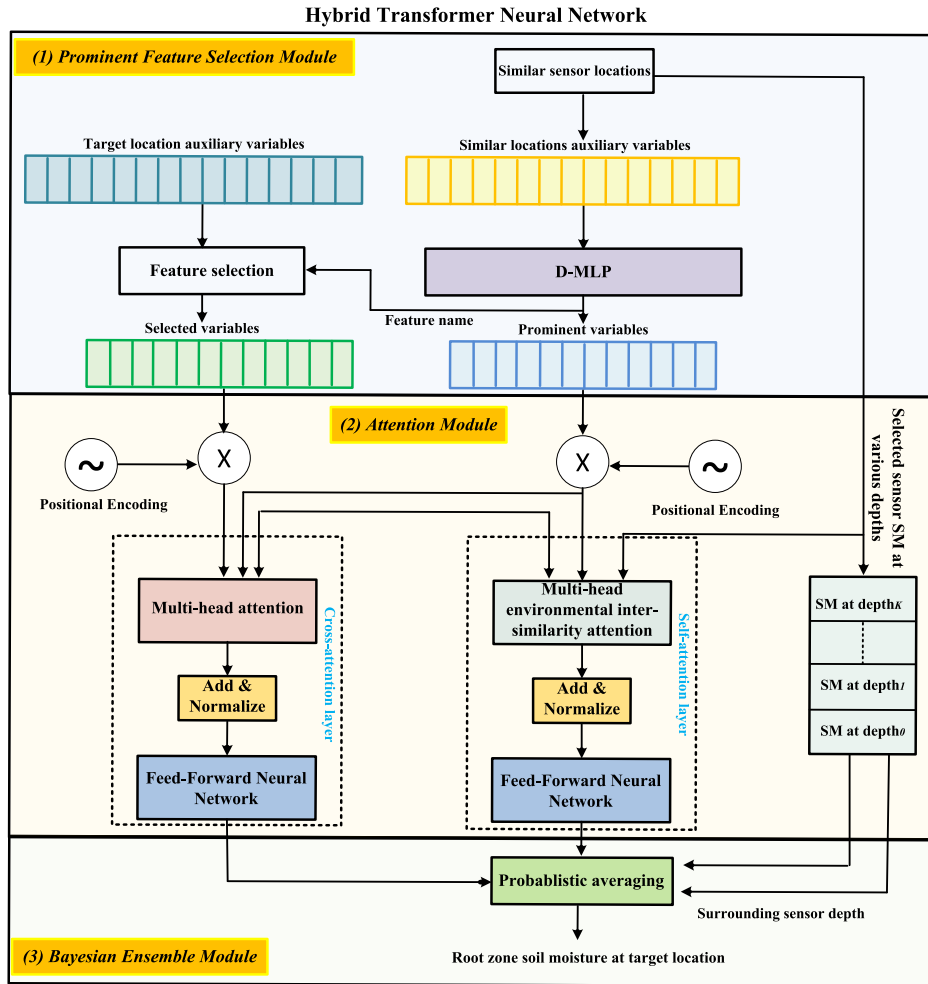
FIGURE 4. Root zone soil moisture estimation using the hybrid transformer neural network (hybrid TNN). The hybrid TNN has three modules: (1) Prominent feature selection module: from the similar SSM sensor locations, the D-MLP (violet box) selects prominent predictor variables from auxiliary-RZSM variables. The selected feature name is used to select the same feature from the target (white box); (2) Attention module: the selected variables undergo position encoding to track the order of the selected variable sequence. The position encoded selected features from target and sensor sites are provided to the multi-head attention module (brown box). The module finds the relative relationship between the selected sensor and target location data. The multi-head environmental inter-similarity attention module (light blue box) finds the relative relationship between the multi-location RZSM and prominent predictor variables from sensor sites; (3) Bayesian ensemble module: performs a Bayesian average of multi-sensor RZSM using the conditional probability (green box) generated based on the attention module output to estimate target RZSM.

features at G locations. The relative relationship between c_h^s and $\{c_1^s, \ldots, c_G^s\}$ is $\{r_{h\to 1}, \ldots, r_{h\to G}\}$. For any location $u \in g$, this can be expressed as,

$$r_{h\to u}^s(t) = \frac{e^{\frac{min(c_h^s(t), c_u^s(t))}{max(c_h^s(t), c_u^s(t))}}}{\sum_{g=1}^{G} e^{\frac{min(c_h^s(t), c_g^s(t))}{max(c_h^s(t), c_g^s(t))}}} \forall s \in \{1, \ldots, S\},$$
$$t \in \{1, \ldots, T\}. \quad (3)$$

The relative relationship in Eq. (3) is used to get the transformed input features from g locations '$\tilde{c_g^s}(t)$' as,

$$\tilde{c_g^s}(t) = \sum_{g=1}^{G} r_{h\to g}^s(t) c_g^s(t) \forall s \in \{1, \ldots, S\}, t \in \{1, \ldots, T\}. \quad (4)$$

Transforming the RZSM at g locations in Eq. (2) using the transformed auxiliary-RZSM variables in Eq. (4) as,

$$\hat{y_g}(t) = fp_g(\tilde{c_g^s}(t)) \forall P_g, s \in \{1, \ldots, S\}, t \in \{1, \ldots, T\}, \quad (5)$$

where $\hat{y_g}(t)$ is the predicted RZSM. The objective of each hybrid TNN predictor neuron, denoted as P_g, is to find out the relationship between $\tilde{c_g^s}(t)$ and $\hat{y_g}(t)$. To ensemble the relative SM at g locations for getting the SM at target location, the Bayesian average is used. The ensemble SM prediction, given the data $\tilde{c_g^s}(t)$, is

$$y^{en}(t) = \sum_{g=1}^{G} p(\hat{y}|P_g, \tilde{c_g^s})(t) p(P_g|\tilde{c_g^s})(t) y_g(t)$$
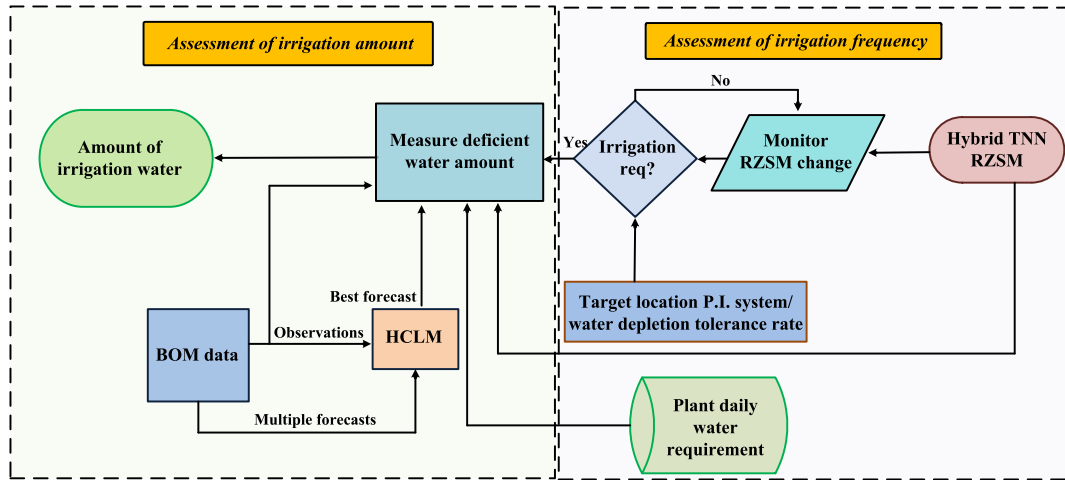
FIGURE 5. The Irrigation processor with two main parts: (a) Irrigation frequency assessment module (light violent square with dashed black outline) and (b) Irrigation amount assessment module (light green square with dashed black outline). The irrigation frequency assessment module examines if irrigation is required using hybrid TNN predicted RZSM (brown ellipse) and water depletion tolerance (dark blue rectangle) data. The irrigation amount assessment module subtracts the water available from BOM rainfall data (dark blue square) and hybrid TNN RZSM from plant water requirement (green cylinder) data.

$$\forall\, t \in \{1, 2, 3, \ldots, T\}, \tag{6}$$

where $y^{en}(t)$ represent the RZSM at the location $h \neq g$ for $t \in \{1, \ldots, T\}$ time instants. $y_g(t)$ is the actual RZSM measured by the sensors at g locations. $p(\hat{y}|P_g, \tilde{c}_g^s)$ is the SM PDF based on P_g alone, estimated from training data, and $p(P_g|\tilde{c}_g^s)$ is the posterior probability of predictor P_g being correct for the given training data, $c_g^s(t)$. Next, the estimated RZSM ($y^{en}(t)$) is provided to the irrigation processor for further processing.

3) IRRIGATION PROCESSOR

Fig. 5 illustrate the proposed irrigation processor. The irrigation frequency module in the irrigation processor decides whether irrigation is required or not based on the water depletion tolerance rate ($R(t)$) for each irrigation type. The $R(t)$ value is calculated using [43] as follows,

$$R(t) = P_{wr}(t) - \left(\frac{P_{wr}(t) \times DT}{100}\right) \ \forall\, t \in \{1, 2, 3, \ldots, T\}, \tag{7}$$

where $P_{wr}(t)$ is the daily water requirement of the plant and DT is the soil water depletion tolerance by the PI system. The $P_{wr}(t)$ should not drop below $R(t)$ to maintain water levels above wilting point.

The DSS used for PI knows the irrigation requirements in the farm using Eq. (7) and use this information for controlling an automatic irrigation system for precise application of water to plants. The main type of irrigation system used for PI is drip irrigation. Ideally, for drip irrigation systems, the DT should be in the range of 20 to 25 [43].

The proposed irrigation processor decides on when irrigation should occur as follows,

$$\forall\, y^{en}(t) \le R(t) : \text{Irrigation required} \tag{8}$$

$$\forall\, y^{en}(t) > R(t) : \text{Irrigation not required.}$$

If irrigation is required, the amount of water to be given through irrigation is evaluated next. The amount of water to be provided through irrigation is calculated as

$$A(t) = P_{wr}(t) - (y^{en}(t) + W(t)) \ \forall\, t \in \{1, 2, 3, \ldots, T\}, \tag{9}$$

where $A(t)$ is the amount of irrigation water, $P_{wr}(t)$ is the daily water requirement of the plant, $y^{en}(t)$ is the hybrid TNN estimated RZSM, and $W(t)$ is the estimated water available from rainfall for the selected day using [44]. The proposed model is tested in Section III.

III. RESULTS AND DISCUSSION

In this section, simulations are performed to evaluate the effectiveness and potentialities of the proposed hybrid TNN for RZSM and irrigation predictions at three different test sites in Melbourne, (1) Alexandra Gardens, (2) Batman Park, and (3) Fawkner Park. Both quantitative and resource conservation efficiency comparisons are conducted with the Multi-head TNN [25], LSTM-Technique [32] and Hybrid GRU [27].

A. QUANTITATIVE PERFORMANCE EVALUATION

To demonstrate the effectiveness of the hybrid TNN, we conduct a comparative analysis between predicted and actual values obtained from soil sensors at various soil depths across the three test locations. Figures 6 (a)-(c) depict the percentage change in average predicted soil moisture across eight layers relative to the actual values. Positive and negative changes along the vertical axis signify over-prediction and under-prediction, respectively. Over-predictions of RZSM can lead to inadequate irrigation, while under-predictions

(a) Alexandra Garden, Melbourne

(b) Batman Park, Melbourne

(c) Fawkner Park, Melbourne
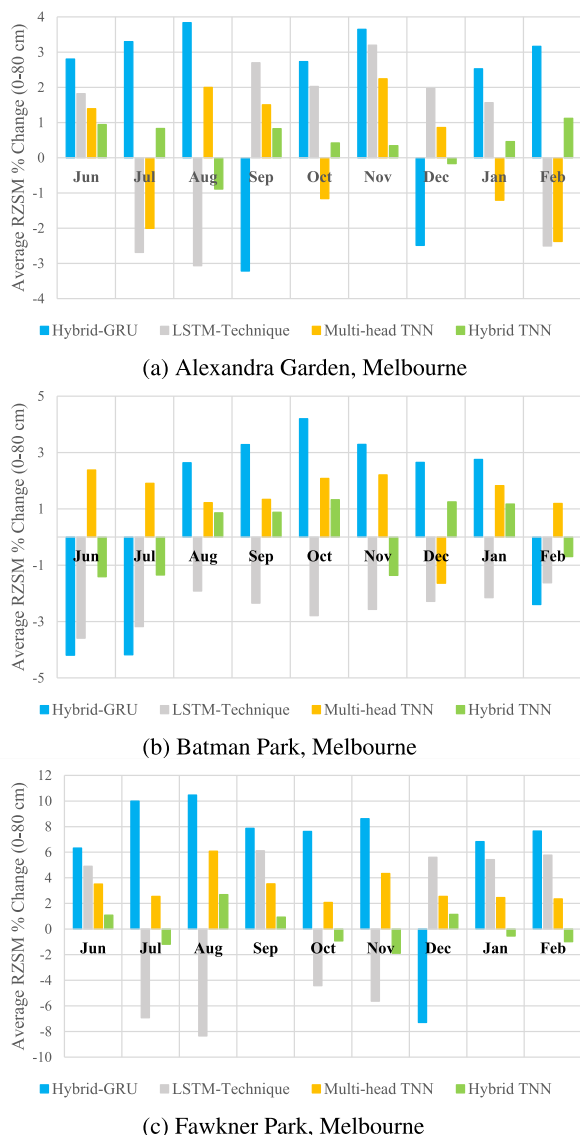
FIGURE 6. Comparative analysis of percentage changes in average predicted soil moisture across eight layers, relative to actual values, for Hybrid GRU [27] (blue dotted line with x marker), LSTM-Technique (red semicolon line) [32], Multi-head TNN [25] (black dashed line), and Hybrid TNN from June 2020 to February 2021 at three locations: (a) Alexandra Gardens, (b) Batman Park, and (c) Fawkner Park. Notably, the Hybrid TNN prediction (green line) exhibits the least deviation from the actual values.

TABLE 1. Time complexity comparison of Hybrid TNN, Multi-head TNN [25], Hybrid GRU [27] and LSTM-Technique [32].

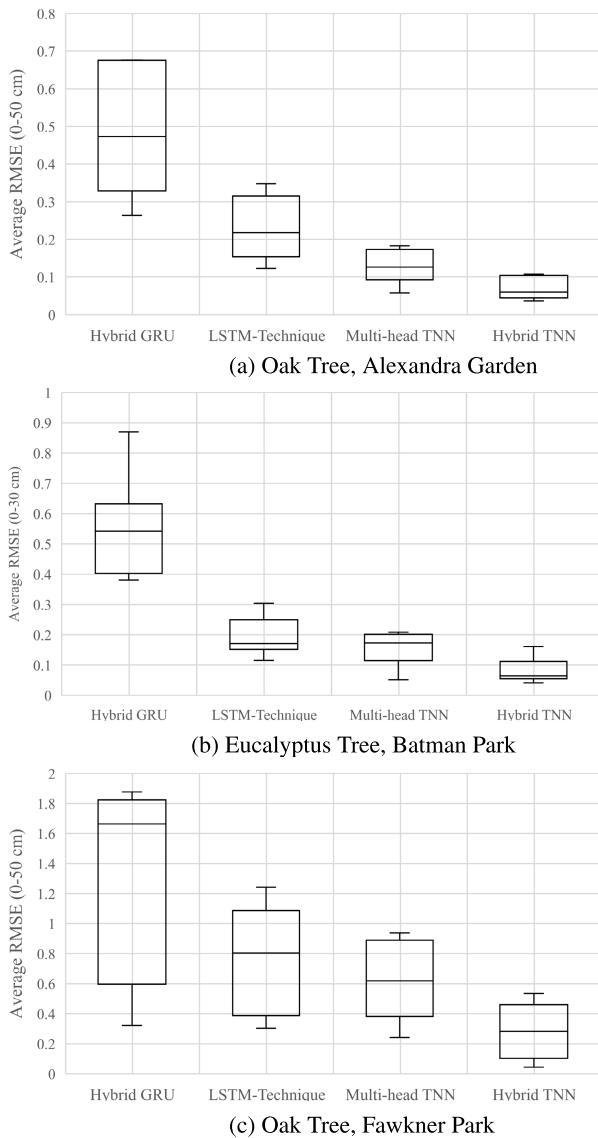| Time	Hybrid GRU	LSTM-Technique	Multi-head TNN	Hybrid TNN
Train (min)	27.73	40.62	20.53	16.79
Test (s)	1.25	1.60	0.97	0.83

TABLE 2. RZSM prediction accuracy comparison of the proposed Hybrid TNN, Multi-head TNN [25], Hybrid GRU [27], and LSTM-Technique [32] at eight soil layers on the RZSM dataset with three test locations data.

Depth	Model	Performance Indices for the Test Data			
		NSE	R^2	NMBE	SD
0-10 cm	Hybrid GRU	0.6945	0.9633	-0.1502	1.3626
	LSTM-Technique	0.7658	0.9721	-0.0620	0.9045
	Multi-head TNN	0.8014	0.9851	-0.0427	0.5420
	Hybrid TNN	0.8527	0.9913	-0.0252	0.3006
10-20 cm	Hybrid GRU	0.7357	0.9783	-0.0873	1.5981
	LSTM-Technique	0.8493	0.9818	-0.0397	0.9259
	Multi-head TNN	0.8623	0.9825	-0.0271	0.5981
	Hybrid TNN	0.9012	0.9879	-0.0156	0.3364
20-30 cm	Hybrid GRU	0.6580	0.9368	-0.1490	1.6419
	LSTM-Technique	0.7716	0.9475	-0.0812	0.9612
	Multi-head TNN	0.8148	0.9748	-0.0542	0.6485
	Hybrid TNN	0.8963	0.9817	-0.0320	0.3841
30-40 cm	Hybrid GRU	0.5708	0.9679	-0.0926	1.6569
	LSTM-Technique	0.9017	0.9715	-0.0577	0.9750
	Multi-head TNN	0.9194	0.9797	-0.0319	0.6672
	Hybrid TNN	0.9486	0.9981	-0.0109	0.4185
40-50 cm	Hybrid GRU	0.7016	0.9528	-0.0532	1.6950
	LSTM-Technique	0.9098	0.9643	-0.0156	1.0070
	Multi-head TNN	0.9325	0.9758	-0.0109	0.6951
	Hybrid TNN	0.9627	0.9826	-0.0073	0.4450
50-60 cm	Hybrid GRU	0.7764	0.9283	-0.0299	1.9459
	LSTM-Technique	0.9389	0.9542	-0.0207	0.9675
	Multi-head TNN	0.9209	0.9728	-0.0152	0.7118
	Hybrid TNN	0.9950	0.9973	-0.0079	0.4071
60-70 cm	Hybrid GRU	0.6998	0.9017	-0.0229	2.1342
	LSTM-Technique	0.8697	0.9218	-0.0125	1.0888
	Multi-head TNN	0.8752	0.9408	-0.0116	0.7908
	Hybrid TNN	0.8967	0.9640	-0.0089	0.4525
70-80 cm	Hybrid GRU	0.7789	0.9463	-0.6512	2.4491
	LSTM-Technique	0.8901	0.9623	-0.4531	1.2384
	Multi-head TNN	0.9039	0.9691	-0.2522	0.8622
	Hybrid TNN	0.9121	0.9729	-0.0895	0.4809
Average	Hybrid GRU	0.7020	0.9469	-0.1545	1.8105
	LSTM-Technique	0.8621	0.9594	-0.0928	1.0085
	Multi-head TNN	0.8788	0.9726	-0.0557	0.6895
	Hybrid TNN	**0.9207**	**0.9845**	**-0.0247**	**0.4031**

Note: The quantitative performance of these models is evaluated Nash Suttcliff coefficient of efficiency (NSE), determination coefficient (R^2), and normalized mean bias error (NMBE). The NSE is commonly used to assess the performance of hydrological predictions. NSE values closer to one suggest the prediction model is a better predictor than the mean of the actual values. The R^2 values nearer to 1 indicate a highly reliable model for future predictions. NMBE captures the average bias in the RZSM prediction. Positive NMBE represents that the RZSM is overestimated. Standard deviation (SD) measures the dispersion of predictions around the mean. A higher SD suggests greater uncertainty in the predictions.

can result in irrigation flooding by automatic irrigation systems. The visualizations in Figures 6 (a)-(c) highlight that the predictions by the hybrid TNN closely align with the actual RZSM, outperforming hybrid GRU [27], LSTM-Technique [32], and Multi-head TNN [25]. This suggests a higher level of reliability in the hybrid TNN model, which is crucial for preventing both under-irrigation and potential irrigation flooding by automatic irrigation systems. Additionally, Table 1 presents the training and testing times for the four comparison models. Notably, the proposed hybrid TNN demonstrates significantly lower training and testing times compared to the other three competing models, indicating reduced time and computational complexity.

Further quantitative measurements are considered to synthesize the model's performance effectiveness over eight months for three stations. Table 2 shows the performance comparison of the hybrid GRU [27], LSTM-Technique [32], Multi-head TNN [25] and hybrid TNN across eight different soil layers on the RZSM dataset with the three test locations data using Nash Suttcliff coefficient of efficiency (NSE), determination coefficient (R^2), normalized mean bias error (NMBE) and Standard deviation (SD). Significantly, the proposed hybrid TNN demonstrates superior performance compared to the hybrid GRU, LSTM-Technique, and Multi-head TNN. This is highlighted by the hybrid TNN's NSE value, which is closest to 1, indicating a significantly higher relative accuracy in predicting RZSM. Specifically, the proposed hybrid TNN has R^2 values closer to 1, indicating a highly reliable prediction model. The negative NMBE values indicate that all the four models ([25], [32], and proposed hybrid TNN) do not overfit the dataset. Lower SD values in Table 2 by the proposed model suggest reduced uncertainty compared to the other comparison models.

FIGURE 7. Comparison of RMSE average over the active root zone depths of target tree by the Hybrid GRU [27], the LSTM-Technique [32], Multi-head TNN [25], and the proposed hybrid TNN for: (a) Oak Tree (0-50 cm), Alexandra Garden, Melbourne, (b) Eucalyptus Tree (0-30 cm), Batman Park, Melbourne, and (c) Oak Tree (0-50 cm), Fawkner Park, Melbourne from June 2020 to February 2021.

Figs. 7 (a)-(c) compares the average root mean square error (RMSE) over the active root zone depths from June 2020 to February 2021 at three test sites. Lower RMSE implies higher prediction accuracy. Fig. 7 (a) illustrates the RZSM prediction error for an oak tree at Alexandra Gardens, Melbourne. The oak tree's active root zone lies in the 0-50 cm layer [45], [46]. Fig. 7 (b) illustrates the RZSM prediction error for a eucalyptus tree at Batman Park, Melbourne. Eucalyptus trees have shallow roots and grow up to 20-30 cm soil depth [45], [46]. Fig. 7 (c) illustrates the RZSM prediction error for an oak tree at Fawkner Park, Melbourne. In Figs. 7 (a)-(c), the lowest prediction error is indicated by the proposed hybrid TNN in all three locations. In addition to the RMSE, the vertical error bars in Figs. 7 (a)-(c) illustrate the standard

TABLE 3. Total comparative water savings in Kilolitre (KL) by by Hybrid TNN based irrigation against Multi-head TNN [25], Hybrid GRU [27] and LSTM-Technique [32] across all three test locations during 2020-2021 using recycled water.

Saving against:	Water saving/tree/year (KL)	Water saving/total area/year (KL)
Hybrid GRU	8.24	60,325.04
LSTM-Technique	8.04	58,860.84
Multi-head TNN	7.29	53,370.09
Average	7.86	57,518.66

Note: The water cost calculation is based on the 2020/2021 class B and C recycled water tariff rate from Western Waters, Victoria, Australia. https://www.westernwater.com.au/our-services/recycled-water/class-b-c-recycled-water. The energy cost calculation is based on the 2020/2021 public unmetered supplies energy tariff rate from CitiPower, Victoria, Australia. https://www.aer.gov.au/networks-pipelines/determinations-access-arrangements/pricing-proposals-tariffs/citipower-annual-pricing-2020. It is assumed that the pump capacity is 10 kW, under a constant rate of 65 L/s.

TABLE 4. Total comparative cost savings in Australian Dollar (AUD) by Hybrid TNN based irrigation against Multi-head TNN [25], Hybrid GRU [27] and LSTM-Technique [32] across all three test locations during 2020-2021 using recycled water.

Saving against:	Cost saving/tree/year (AUD)	Cost saving/total area/year (AUD)
Hybrid GRU	2.91	21,304.11
LSTM-Technique	2.69	19,693.49
Multi-head TNN	2.23	16,325.83
Average	2.80	19,107.81

Note: The water cost calculation is based on the 2020/2021 class B and C recycled water tariff rate from Western Waters, Victoria, Australia. https://www.westernwater.com.au/our-services/recycled-water/class-b-c-recycled-water. The energy cost calculation is based on the 2020/2021 public unmetered supplies energy tariff rate from CitiPower, Victoria, Australia. https://www.aer.gov.au/networks-pipelines/determinations-access-arrangements/pricing-proposals-tariffs/citipower-annual-pricing-2020. It is assumed that the pump capacity is 10 kW, under a constant rate of 65 L/s.

deviation of prediction accuracy by each model. The error bars indicate a less standard deviation of prediction for the proposed hybrid TNN compared to hybrid GRU [27], LSTM-Technique [32], and Multi-head TNN [25].

The lower RMSE of hybrid TNN also indicates its usability in addressing the performance drop in existing PI decision support systems [7] due to the RZSM estimation error accumulations than hybrid GRU [27], LSTM-Technique [32], and Multi-head TNN [25]. The resource conservation efficiency evaluation of the hybrid GRU [27], LSTM-Technique [32], Multi-head TNN [25] and hybrid TNN-based irrigation schedules are conducted further in Section III-B.

B. RESOURCE CONSERVATION EFFICIENCY ASSESSMENT

In this section, we present the drip irrigation simulation results of the hybrid GRU [27], LSTM-Technique [32], Multi-head TNN [25] and proposed hybrid TNN. As discussed before drip irrigation is a widely adopted irrigation system for PI. The irrigation is simulated from June 2020 to February 2021 for three test locations. The water balance, water savings, and cost savings are evaluated for resource conservation efficiency performance comparisons between the hybrid GRU [27], LSTM-Technique [32], Multi-head TNN [25] and proposed hybrid TNN.

Fig. 8 illustrates the water balance of the drip irrigation schedules produced using the three RZSM predictions. Drip irrigation systems are usually designed to keep root zone moisture close to the optimum level by daily moisture evaluation. Irrigation will be applied when the root zone

(a) Oak Tree, Alexandra Garden, Melbourne

(b) Eucalyptus Tree, Batman Park, Melbourne

(c) Oak Tree, Fawkner Park, Melbourne

FIGURE 8. Comparison of irrigation water balance by Hybrid GRU [27] (blue semicolon line with x marker), LSTM-Technique [32] (grey dashed line), (3) Multi-head TNN [25] (green line) and (4) Hybrid TNN (red line) at (a) Alexandra Garden, (b) Batman Park, and (c) Fawkner Park. The hybrid TNN line is closer to zero (most optimum irrigation) than the other models.

water depletes below 20% of the requirement [43]. The daily water depletion tolerance for the trees on the three sites is 13.52 mm, 9 mm, and 21.03 mm.

The values are calculated by substituting daily water requirement of the tree species from literature ([36], [45]) in Eq. (7). All four models, schedule irrigation to meet the plant water requirement post subtracting the daily water obtained from rainfall. The Melbourne (Olympic Park), BOM, Australia weather station data is used to schedule irrigation at Alexandra Gardens and Batman Park for supplementing rainfall water. The Hawthorn (Scotch College), BOM, Australia weather station data is used for Fawkner Park irrigation.

The irrigation water balance by the hybrid GRU [27], LSTM-Technique [32], Multi-head TNN [25] and hybrid

TNN irrigation scheduling systems is shown in Fig. 8 (a)-(c). The proximity of each model's water balance graph to zero indicates higher closeness between predicted and actual irrigation amounts. The plant irrigation water requirement at each test site is closely met by the hybrid TNN compared to hybrid GRU, LSTM-Technique, and Multi-head TNN. Fig. 8 (a)-(c) illustrate that more irrigation water is wasted by hybrid GRU [27], LSTM-Technique [32], and Multi-head TNN [25] compared to the proposed hybrid TNN.

To further quantify the water and cost saved by the proposed hybrid TNN, the irrigation water amount by the three competing models is compared for the three test locations. All three test locations use recycled water for irrigation. Table 3 shows that the proposed hybrid TNN conserved 60,325.04 KL, 58,860.84 KL, and 53,370.09 KL of water compared to hybrid GRU [27], LSTM-Technique [32], and Multi-head TNN [25] respectively in total over the three test locations. Next, the irrigation cost calculation for all the four models is carried out through a comprehensive approach involving three main steps. Firstly, the irrigation water cost for each model is determined by multiplying the amount of water utilized by the respective model with the corresponding water tariff rate (referenced in the footnote of Table 4). Secondly, the power consumption associated with pumping irrigation water for each model is quantified by multiplying the energy used with the energy tariff rate (referenced in the footnote of Table 4). Finally, the total cost for each model is derived by summing both the water cost and the energy cost. Overall, Table 4 shows that hybrid TNN saved 21,304.11 AUD compared to hybrid GRU [27], 19,693.49 AUD compared to LSTM-Technique [32] and 16,325.83 AUD compared to Multi-head TNN [25] in total cost savings over the three test locations for a duration of one year.

The average savings by hybrid TNN is 10.846% water and 10.339% cost compared to the comparison models. From the results in this section, it can be concluded that the proposed hybrid TNN attains a more precise water balance than hybrid GRU [27], LSTM-Technique [32], and Multi-head TNN [25], thus reducing water loss and increasing irrigation profitability.

IV. CONCLUSION

Irrigation traditionally complements rainfall, but a significant portion of rainwater is lost through deep percolation and run-off. Theoretical studies emphasize that water beyond the root zone is unusable for plants. Therefore, precision irrigation (PI) should focus on the root-zone soil moisture (RZSM). This paper introduces a hybrid TNN for RZSM estimation to provide decision support for PI. The model incorporates a dynamic MLP (D-MLP) network layer to select nearby soil moisture (SM) sensor locations data aligned with the target location. This selected data then passes through a proposed dual attention block and a Bayesian layer to estimate RZSM, subsequently informing irrigation schedules. Performance evaluation demonstrates the superior

accuracy of the proposed model-based RZSM compared to existing state-of-the-art deep learning models. Furthermore, simulation results reveal increased water and cost savings with the proposed hybrid TNN-based irrigation compared to the state-of-the-art competing models.

REFERENCES

[1] C. Carranza, C. Nolet, M. Pezij, and M. van der Ploeg, "Root zone soil moisture estimation with random forest," *J. Hydrol.*, vol. 593, Feb. 2021, Art. no. 125840.

[2] Y. Gamal, A. Soltan, L. A. Said, A. H. Madian, and A. G. Radwan, "Smart irrigation systems: Overview," *IEEE Access*, early access, Mar. 2, 2023, doi: 10.1109/ACCESS.2023.3251655.

[3] B. Kashyap and R. Kumar, "Sensing methodologies in agriculture for soil moisture and nutrient monitoring," *IEEE Access*, vol. 9, pp. 14095–14121, 2021.

[4] M. Link, M. Drusch, and K. Scipal, "Soil moisture information content in SMOS, SMAP, AMSR2, and ASCAT level-1 data over selected in situ sites," *IEEE Geosci. Remote Sens. Lett.*, vol. 17, no. 7, pp. 1213–1217, Jul. 2020.

[5] Y. Yi, K. Bakian-Dogaheh, M. Moghaddam, U. Mishra, and J. S. Kimball, "Mapping surface organic soil properties in Arctic Tundra using C-band SAR data," *IEEE J. Sel. Topics Appl. Earth Observ. Remote Sens.*, vol. 16, pp. 1403–1413, 2023.

[6] A. Singh, K. Gaurav, G. K. Sonkar, and C.-C. Lee, "Strategies to measure soil moisture using traditional methods, automated sensors, remote sensing, and machine learning techniques: Review, bibliometric analysis, applications, research findings, and future directions," *IEEE Access*, vol. 11, pp. 13605–13635, 2023.

[7] M. Zribi and M. Dechambre, "A new empirical model to retrieve soil moisture and roughness from C-band radar data," *Remote Sens. Environ.*, vol. 84, no. 1, pp. 42–52, Jan. 2003.

[8] M. Sadeghi, M. Tuller, A. W. Warrick, E. Babaeian, K. Parajuli, M. R. Gohardoust, and S. B. Jones, "An analytical model for estimation of land surface net water flux from near-surface soil moisture observations," *J. Hydrol.*, vol. 570, pp. 26–37, Mar. 2019.

[9] T. Wang, T. E. Franz, J. You, M. D. Shulski, and C. Ray, "Evaluating controls of soil properties and climatic conditions on the use of an exponential filter for converting near surface to root zone soil moisture contents," *J. Hydrol.*, vol. 548, pp. 683–696, May 2017.

[10] A. Ritter, F. Hupet, R. Muñoz-Carpena, S. Lambot, and M. Vanclooster, "Using inverse methods for estimating soil hydraulic properties from field data as an alternative to direct methods," *Agricult. Water Manage.*, vol. 59, no. 2, pp. 77–96, Mar. 2003.

[11] D. J. Wilson, A. W. Western, and R. B. Grayson, "A terrain and data-based method for generating the spatial distribution of soil moisture," *Adv. Water Resour.*, vol. 28, no. 1, pp. 43–54, Jan. 2005.

[12] X. Gao, X. Zhao, L. Brocca, D. Pan, and P. Wu, "Testing of observation operators designed to estimate profile soil moisture from surface measurements," *Hydrolog. Processes*, vol. 33, no. 4, pp. 575–584, Feb. 2019.

[13] J. Peng and A. Loew, "Recent advances in soil moisture estimation from remote sensing," *Water*, vol. 9, no. 7, p. 530, Jul. 2017.

[14] S. Chatterjee, A. E. Hartemink, J. Triantafilis, A. R. Desai, D. Soldat, J. Zhu, P. A. Townsend, Y. Zhang, and J. Huang, "Characterization of field-scale soil variation using a stepwise multi-sensor fusion approach and a cost-benefit analysis," *Catena*, vol. 201, Jun. 2021, Art. no. 105190.

[15] E. Santi, S. Paloscia, S. Pettinato, and G. Fontanelli, "Neural network integration of SMAP and Sentinel-1 for estimating soil moisture at high spatial resolution," in *Proc. IEEE Int. Geosci. Remote Sens. Symp.*, Jul. 2021, pp. 6327–6330.

[16] Z. Gu, T. Zhu, X. Jiao, J. Xu, and Z. Qi, "Neural network soil moisture model for irrigation scheduling," *Comput. Electron. Agricult.*, vol. 180, Jan. 2021, Art. no. 105801.

[17] M. Al-Mukhtar, "Modelling the root zone soil moisture using artificial neural networks, a case study," *Environ. Earth Sci.*, vol. 75, no. 15, pp. 1–12, Aug. 2016.

[18] S.-S. Chai, J. Walker, O. Makarynskyy, M. Kuhn, B. Veenendaal, and G. West, "Use of soil moisture variability in artificial neural network retrieval of soil moisture," *Remote Sens.*, vol. 2, no. 1, pp. 166–190, Dec. 2009.

[19] Z. Xu, X. Man, L. Duan, and T. Cai, "Improved subsurface soil moisture prediction from surface soil moisture through the integration of the (de)coupling effect," *J. Hydrol.*, vol. 608, May 2022, Art. no. 127634.

[20] K. Fang, M. Pan, and C. Shen, "The value of SMAP for long-term soil moisture estimation with the help of deep learning," *IEEE Trans. Geosci. Remote Sens.*, vol. 57, no. 4, pp. 2221–2233, Apr. 2019.

[21] P.-W. Liu, R. Bindlish, B. Fang, V. Lakshmi, P. E. O'Neill, Z. Yang, M. H. Cosh, T. Bongiovanni, D. D. Bosch, C. H. Collins, P. J. Starks, J. Prueger, M. Seyfried, and S. Livingston, "Assessing disaggregated SMAP soil moisture products in the United States," *IEEE J. Sel. Topics Appl. Earth Observ. Remote Sens.*, vol. 14, pp. 2577–2592, 2021.

[22] L. He, Y. Cheng, Y. Li, F. Li, K. Fan, and Y. Li, "An improved method for soil moisture monitoring with ensemble learning methods over the Tibetan Plateau," *IEEE J. Sel. Topics Appl. Earth Observ. Remote Sens.*, vol. 14, pp. 2833–2844, 2021.

[23] O. Adeyemi, I. Grove, S. Peets, Y. Domun, and T. Norton, "Dynamic neural network modelling of soil moisture content for predictive irrigation scheduling," *Sensors*, vol. 18, no. 10, p. 3408, Oct. 2018.

[24] N. Sazib, J. Bolten, and I. Mladenova, "Exploring spatiotemporal relations between soil moisture, precipitation, and streamflow for a large set of watersheds using Google Earth Engine," *Water*, vol. 12, no. 5, p. 1371, May 2020.

[25] T.-T.-H. Nguyen, D.-Q. Vu, S. T. Mai, and T. D. Dang, "Streamflow prediction in the Mekong river basin using deep neural networks," *IEEE Access*, vol. 11, pp. 97930–97943, 2023.

[26] T. Sampathkumar, B. J. Pandian, and S. Mahimairaja, "Soil moisture distribution and root characters as influenced by deficit irrigation through drip system in cotton-maize cropping sequence," *Agricult. Water Manage.*, vol. 103, pp. 43–53, Jan. 2012.

[27] J. Yu, X. Zhang, L. Xu, J. Dong, and L. Zhangzhong, "A hybrid CNN-GRU model for predicting soil moisture in maize root zone," *Agricult. Water Manage.*, vol. 245, Feb. 2021, Art. no. 106649.

[28] P. Pokhrel, E. Ioup, J. Simeonov, M. T. Hoque, and M. Abdelguerfi, "A transformer-based regression scheme for forecasting significant wave heights in oceans," *IEEE J. Ocean. Eng.*, vol. 47, no. 4, pp. 1010–1023, Oct. 2022.

[29] H. Yin, X. Zhang, F. Wang, Y. Zhang, R. Xia, and J. Jin, "Rainfall-runoff modeling using LSTM-based multi-state-vector sequence-to-sequence model," *J. Hydrol.*, vol. 598, Jul. 2021, Art. no. 126378.

[30] S. Yang, X. Yu, and Y. Zhou, "LSTM and GRU neural network performance comparison study: Taking yelp review dataset as an example," in *Proc. Int. Workshop Electron. Commun. Artif. Intell. (IWECAI)*, Shanghai, China, Jun. 2020, pp. 98–101.

[31] B. Lim, S. Ö. Arık, N. Loeff, and T. Pfister, "Temporal fusion transformers for interpretable multi-horizon time series forecasting," *Int. J. Forecasting*, vol. 37, no. 4, pp. 1748–1764, Oct. 2021.

[32] K. Wasayangkool, S. Dangsri, E. Chootieng, K. Luangampol, K. Srisomboon, and W. Lee, "Moisture prediction system with LSTM technique for cactus farm," in *Proc. 18th Int. Conf. Electr. Eng./Electron., Comput., Telecommun. Inf. Technol. (ECTI-CON)*, May 2021, pp. 144–147.

[33] S. Chaudhari, V. Mithal, G. Polatkan, and R. Ramanath, "An attentive survey of attention models," *ACM Trans. Intell. Syst. Technol.*, vol. 12, no. 5, pp. 1–32, Oct. 2021.

[34] N. Madhukumar et al., "3-D bi-directional LSTM for satellite soil moisture downscaling," *IEEE Trans. Geosci. Remote Sens.*, vol. 60, pp. 1–18, Dec. 2022, Art. no. 5414018.

[35] L. J. Wilson, S. Beauregard, A. E. Raftery, and R. Verret, "Calibrated surface temperature forecasts from the Canadian ensemble prediction system using Bayesian model averaging," *Monthly Weather Rev.*, vol. 135, no. 4, pp. 1364–1385, Apr. 2007.

[36] The Victorian Government City of Melbourne Open Data Portal. (2021). *Soil Sensor Readings*. Melbourne, VIC, Australia, Accessed: Jan. 28, 2022. [Online]. Available: https://data.melbourne.vic.gov.au/Environment/Soil-Sensor-Readings/mv4n-8k4v

[37] The Victorian Government City of Melbourne Open Data Portal. (2021). *Soil Sensor Locations*, Melbourne, VIC, Australia. Accessed: Jan. 28, 2022. [Online]. Available: https://data.melbourne.vic.gov.au/Environment/Soil-Sensor-Locations/dxvp-runr

[38] The Victorian Government City of Melbourne Open Data Portal. (2021). *Soil Types by Area (Urban Forest)*. Melbourne, VIC, Australia. Accessed: Jan. 28, 2022. [Online]. Available: https://data.melbourne.vic.gov.au/Environment/Soil-types-by-area-Urban-Forest-/t3zn-qgfx

[39] The Bureau of Meteorology. (2015). *Meteorological Verification Data Technical Reference*. Accessed: Feb. 28, 2020. [Online]. Available: https://data.gov.au/search?q=Rainfall%20and%20temperature%20forecast%20and%20observations

[40] F. O. Nachtergaele, O. Spaargaren, J. A. Deckers, and B. Ahrens, "New developments in soil classification: World reference base for soil resources," *Geoderma*, vol. 96, no. 4, pp. 345–357, Jul. 2000.

[41] J. D. Olden and D. A. Jackson, "Illuminating the 'black box': A randomization approach for understanding variable contributions in artificial neural networks," *Ecolog. Model.*, vol. 154, nos. 1–2, pp. 135–150, Aug. 2002.

[42] N. Aloysius, M. Geetha, and P. Nedungadi, "Incorporating relative position information in transformer-based sign language recognition and translation," *IEEE Access*, vol. 9, pp. 145929–145942, 2021.

[43] J. Brenner, "Natural resources conservation service," in *National Engineering Handbook: Irrigation Guide*, vol. 652. Washington, DC, USA: United States Department of Agriculture, Sep. 1997, ch. 3, pp. 56–87.

[44] N. Madhukumar, E. Wang, Y.-F. Zhang, and W. Xiang, "Consensus forecast of rainfall using hybrid climate learning model," *IEEE Internet Things J.*, vol. 8, no. 9, pp. 7270–7278, May 2021.

[45] E. M. O'Loughlin and E. K. S. Nambiar, "Plantations, farm forestry, and water: A discussion paper," in *Proc. Nat. Workshop*, Melbourne, VIC, Australia, Jun. 2000, pp. 1–25.

[46] G. M. Moore and A. Chandler, "The potential of yellow gum (Eucalyptus leucoxylon F. Muell.) as an urban street tree: An assessment of species performance in the city of greater Melbourne, Australia," *Arboriculture Urban Forestry*, vol. 49, no. 1, pp. 16–37, Jan. 2023.

YVETTE EVERINGHAM is currently a Specialist in multi-model data fusion, who is dedicated to identifying strategies that will deliver better student learning outcomes in STEM education and researching AgTech solutions to help agricultural industries increase profits with a smaller environmental footprint under challenging climates. Currently, she holds positions as the Director of the Agriculture, Technology and Adoption Centre (AgTAC) and a Professor in data science with James Cook University with special interests in wavelet methods for data compression. Her previous positions include a Climate Impacts Scientist (CSIRO), the Associate Dean Graduate Research Studies (JCU), the Focus Area Chair of Agricultural Weather and Climate Services (World Meteorological Organization, Geneva), and an Associate Editor of the journal of *Agronomy for Sustainable Development*. During her career, she has been awarded $20 M to support her and her teams' research activities and has produced over 100 peer reviewed publications with more than 2300 citations. In 2008, she was awarded the coveted researcher of the year award by Sugar Research Australia.

NEETHU MADHUKUMAR (Member, IEEE) received the bachelor's and master's degrees in electronics and communication engineering from the University of Kerala, in 2012 and 2015, respectively, and the Ph.D. degree from the College of Science and Engineering, James Cook University (JCU), Australia, in 2023. She was part of the Internet of Things Research Group and is a Peer-Assisted Learning Advisor and at JCU. Currently, she is working as a sessional academic with the Department of Electrical and Computer Systems Engineering, Monash University, Australia. Previously, she was involved in teaching the subject of random processes and applications to undergraduate students with the College of Engineering Trivandrum as part of the Government of Kerala project "Step4U" for a year. As part of the master's research, she was with the National MEMS Design Laboratory, College of Engineering, Trivandrum, and built a structural health monitoring system using MEMS-based wireless sensors. She completed in-plant training with Indian Space Research Organization, in 2014. She is currently a Certified Expert in AI and geospatial analysis from organizations, like Microsoft and Geoscience Australia. Her research interests include wireless sensor networks, 1D/2D/3D data analysis, deep learning, and the Internet of Things. She was a recipient of the JCU Postgraduate Research Scholarship and the All India Council for Technical Education's GATE Scholarship.

ERIC (GENGKUN) WANG (Member, IEEE) received the B.Eng. degree in mechanical engineering and the M.Eng. degree in mechatronic engineering from the University of Science and Technology, Beijing, China, in 2006 and 2009, respectively, and the Ph.D. degree in telecommunications engineering from the University of South Queensland, Australia. He was a Postdoctoral Research Fellow with the School of Electrical and Mechanical, USQ, for two and a half years. He has authored more than 20 high quality articles and participated in many national and international research projects. He received the Best Paper Award from the IEEE Wireless Communications and Networking Conference, Cancun, Mexico, in 2011.

WEI XIANG (Senior Member, IEEE) is currently the Cisco Research Chair of AI and IoT and the Director of the Cisco-La Trobe Centre for AI and IoT, La Trobe University. Previously, he was the Foundation Chair and the Head of the Discipline of IoT Engineering, James Cook University, Cairns, Australia. Due to his instrumental leadership in establishing Australia's first accredited Internet of Things Engineering Degree Program, he was inducted into Pearcy Foundation's Hall of Fame, in October 2018. His research interests include the Internet of Things, wireless communications, machine learning for IoT data analytics, and computer vision. He is also a TEDx Speaker and an elected fellow of the IET, U.K., and Engineers Australia. He received the TNQ Innovation Award, in 2016, Pearcey Entrepreneurship Award, in 2017, and Engineers Australia Cairns Engineer of the Year, in 2017. He was a co-recipient of four Best Paper Awards at WiSATS'2019, WCSP'2015, IEEE WCNC'2011, and ICWMC'2009. He has been awarded several prestigious fellowship titles. He was named a Queensland International Fellow (2010–2011) by the Queensland Government of Australia, an Endeavour Research Fellow (2012–2013) by the Commonwealth Government of Australia, a Smart Futures Fellow (2012–2015) by the Queensland Government of Australia, and a JSPS Invitational Fellow jointly by the Australian Academy of Science and Japanese Society for Promotion of Science (2014–2015). He was the Vice Chair of the IEEE Northern Australia Section, from 2016 to 2020. He is currently an Associate Editor of IEEE Communications Surveys & Tutorials, IEEE Transactions on Vehicular Technology, IEEE Internet of Things Journal, IEEE Access, and *Scientific Reports* (Nature). He has published over 300 peer-reviewed articles, including three books and 220 journal articles. He has severed in a large number of international conferences in the capacity for the general co-chair, the TPC co-chair, and the symposium chair.

● ● ●